Supplementary material

Fani Maoré, a new "young HIMU" volcano with extreme geochemistry

Catherine Chauvel*, Edward C. Inglis‡, Pamela Gutierrez, Tu-Han Luu, Pierre Burckel and Pascale Besson

- Supplementary text : analytical methods
- Supplementary figures 1 to 6
- Supplementary tables S1 to S4 (excel file)

Analytical methods

Major and trace elements

Prior to whole-rock major- and trace-element analyses, any obvious altered part was removed from the investigated rock specimens. Samples were then washed twice with Milli-Q water in an ultrasonic bath. After drying in an oven, samples were crushed to coarse chips and powdered to flour-like consistency using an agate ball mill mortar.

Major elements were analyzed by XRF on the "Rayons X"- Université Paris Cité platform, using an X-ray fluorimeter Epsilon 3xl (Malvern-Panalytical) equipped with an Ag X-ray tube operating under He flow. To optimize the quality of the data, four measuring conditions were used: 5 kV– 60 µA without filter for the analysis of Na, Mg, Al and Si, 10 kV – 30 µA with a 7 µm titanium filter for the analyse of P, 12 kV – 25 µA with a 50µm aluminium filter for the analysis of Ca, K and Ti, and 20 kV – 15 µA with a 200 µm aluminium filter during 120 s for the analysis of Mn and Fe. In order to avoid matrix and grain size effects, all samples were melted into 13 mm homogeneous glass discs prepared by mixing 0.1136 g of rock powder, 1.2312 g of fluxing agent ($LiBO_2/Li_2B_4O_7$) and 0.0187 g of non-wetting agent (LiBr) in a platinum crucible. The mixture was heated to 1050 °C for 25 minutes in an automatic fusion instrument (LeNeo fluxer, Claisse). Calibration curves were obtained from identical beads of 14 geological reference materials (ACE, ANG, BCR-2, BEN, BHVO-2, BIR-1, BXN, DTN, FKN, GSN, MAN, Mica-Fe, Osh BO, UBN) and measured with exactly the same conditions. The curves are perfectly linear over the entire concentration range. Analytical uncertainties (±1σ) are <5% for TiO_2, MnO and Fe_2O_3, 5% for MgO, SiO_2 and CaO, 10% for Al_2O_3, P_2O_5 and K_2O and 20% for Na_2O. All reported data are the means values of 3 duplicate analyses. The BR24 reference material (Chauvel et al. 2011) is used as unknown sample. The data provided were not normalized to anhydrous values and the total Fe content is reported as Fe_2O_3t wt %.

Trace element concentrations were measured at the Institut de Physique du Globe de Paris using an Agilent 8900 ICP-MS-MS. Samples were spiked with indium and subsequently digested in pre-cleaned PFA Teflon beakers using a mix of 2:1 concentrated HF (28M) and HNO_3 (16M) acid for 48 hours before being evaporated to incipient dryness. The decomposed sample residue was then taken up in 6M HCl and treated in an ultrasonic bath for 1-2 hours to ensure total dissolution of any residues that may have formed during the initial digestion phase. After evaporation to dryness, the samples were brought back up in 8M HNO_3 with traces of HF and underwent a few heating (16 hours) and sonication (2-3 hours) cycles until no solid residue could be seen. Samples were then diluted with a factor of 10 000 in 0.5M HNO_3 with traces of HF prior to analysis on the ICP-MS-MS. All reagents used during dissolution, dilution and analysis were distilled to trace metal purity (<ppt level for all elements analysed) and all H_2O was 18.2 MΩ Milli-Q.

The samples were introduced into the ICP-MS-MS via an HF resistant introduction system consisting of a PFA 0.2ml/min concentric nebuliser, a Scott spray chamber and a sapphire torch injector. The collision-reaction cell of the ICP-MS-MS used a 5ml/min He gas flow across the mass range 23 (Na) to 75 (As) in order to remove polyatomic interferences of species occupying the same nominal mass space as the analytes. To correct for matrix and instrumental drift effects, the indium signal from the spike was monitored and used as an internal standard. Samples were bracketed by BE-N standards (one BE-N measurement every two samples) diluted down to the same factor as the samples. The BE-N standard was then used to convert measured counts to absolute sample concentrations using the values recommended by Jochum et al. (2016). The accuracy of the results was evaluated by measuring reference materials BHVO-2, BCR 2 and BR24, whose results are given in **Supporting Table 2**. It is generally better than 5% for most elements.

Radiogenic isotopes (Sr, Nd, Pb and Hf)

Radiogenic isotope measurements were carried out at the Institut de Physique du Globe de Paris. When volcanic glass was available, about 150 mg of fresh glass were hand-picked under a binocular microscope from the coarsely crushed whole rock samples. When no glass was available on the hand samples, we used the rock powders prepared for major and trace elements. All samples were leached prior to dissolution in order to remove any trace of

secondary alteration. For glass samples, 20 minutes of ultrasonic bath washing in milliQ water was followed by a 30-minute leaching in 0.5 M HCl. For rock powders, we applied the same leaching protocol as for glasses. However, for some samples, the measured strontium isotopic composition was suspiciously too radiogenic (1 basanite and 4 phonolites). These five samples were subsequently leached again, using 2M, 4M or 6M HCl to ensure better removal of Sr originating from seawater. Results are given in the Supporting Table 3 together with duplicate analyses of few samples**.** After leaching, all samples were digested in precleaned Teflon® beakers using a 1:3 mix of 16M HNO_3 and 28M HF acid on a hotplate at 125 °C for 48 hours. The isolation of Hf, Pb, Sr and Nd from the sample matrix follows the method previously described in Chauvel et al. (2011) but with few changes. The decomposed sample residue was dissolved in 0.7M Optima grade HBr and centrifuged prior to column chemistry. The first column pass was performed using Teflon® shrink fit columns packed with AG1-X8 (mesh size 100-200) anion exchange resin, with the bulk matrix containing the Sr, Nd and Hf being collected in 0.7M HBr followed by 2M HCl, before elution of the Pb fraction using double distilled 6 M HCl. In order to further purify the Pb fraction this column step was repeated. To purify the matrix cut from the first column, the fraction was passed on a BioRad PolyPrep™ column filled with AG50W-X8 resin with the Hf cut being eluted in 2M HCl + 0.08M HF, the Sr being eluted afterwards in 2M and 3.5M HCl and the REE fraction finally eluted in 6M HCl. The Hf fraction was further purified using small geometry columns packed with ~1 mL of 100-150 μm mesh Ln-spec resin following the procedure detailed by Münker et al. (2001), while the Sr fraction was cleaned up using a column containing ~200 μL Sr-spec resin (50-100 μm) to ensure the total removal of Rb from the Sr cut. Finally, the Nd fraction was quantitively isolated from the matrix cut using an ion chromatography on Ln-spec resin (50-100 μm) in a HCl acid medium, with the eluted Nd cuts being free from isobaric Sm.

Both Pb and Hf isotope measurements were performed using the Neptune or Neptune Plus MC-ICP-MS instrument housed at IPGP. In both cases data were acquired in static mode using either an Elemental Scientific Apex HF or IR to introduce the sample to the plasma as a dry aerosol. In the case of Hf, the Apex HF was used exclusively in conjunction with a Sapphire injector to allow samples to be carried in 0.5M HNO_3 + 0.05M HF. For Pb isotopes, instrumental mass fractionation was corrected by doping the analyte with Tl and performing an empirical normalisation correction using the value of 2.3885 for $^{205}Tl/^{203}Tl$ as described by White et al. (2000). Hafnium isotopic ratios were internally normalised to $^{179}Hf/^{177}Hf = 0.7325$. Instrumental drift was corrected for both Pb and Hf using a sample-standard bracketing

technique. Absolute measured ratios for the standards (NBS 981 for Pb and Hf Ames Grenoble for Hf) were back corrected to known values as is widely accepted, using 16.9435 for $^{206}Pb/^{204}Pb$, 15.5011 for $^{207}Pb/^{204}Pb$, 36.7039 for $^{208}Pb/^{204}Pb$ (Jochum et al., 2011) and 0.282160 for $^{176}Hf/^{177}Hf$ (Chauvel and Blichert-Toft, 2001).

Strontium and Nd isotopes were measured on a Nu Instruments TIMS, at the Institut de Physique du Globe de Paris, using a 5 lines acquisition routine. A single Sr isotope analysis was typically run with ~ 12-13V on $^{88}Sr^{+}$ for 6-7 hours, with ~300 ng of Sr loaded on previously outgassed zone-refined Re single filaments. A single Nd isotope analysis was typically run with ~ 5-7V on $^{144}Nd^{+}$ for 7-8 hours, with 600ng to 800 ng of Nd loaded on previously outgassed zone-refined Re double filaments. Isotope data are then reported as $(^{87}Sr/^{86}Sr)_{multidyn}$ and $(^{143}Nd/^{144}Nd)_{multidyn}$, corresponding to the average of the 4 dynamic $^{87}Sr/^{86}Sr$ or of the 3 dynamic $^{143}Nd/^{144}Nd$. The long-term reproducibility obtained for our Sr (NBS 987) and Nd (Rennes-Ames) standard solutions gives a $(^{87}Sr/^{86}Sr)_{multidyn}$ of 0.7102467 ± 0.0000043 (6.0 ppm, 2 s.d., n = 38) and a $(^{143}Nd/^{144}Nd)_{multidyn}$ of 0.5119537 ± 0.0000022 (4.2 ppm, 2 s.d., n = 31), respectively (Luu et al., 2022). These measured values are in good agreement with the recommended values of Thirlwall (1991) ($^{87}Sr/^{86}Sr$ = 0.710248 ± 0.000011) and Chauvel and Blichert-Toft (2001) ($^{143}Nd/^{144}Nd$ = 0.511961 ± 0.000013).

The overall quality of the data was assessed through total procedural blanks, duplicates and replicates of both individual samples and reference materials (see Supporting Tables 2&3). For all elements the total procedural blanks were negligible relative to sample contribution (Pb < 23 pg, Hf< 126 pg, Sr < 346 pg and Nd < 98 pg).

Barium stable isotopes

Barium isotope measurements were made on freshly picked glasses from the same whole rock samples as described above. Roughly 100 mg of pristine glass was hand-picked under a binocular microscope. Glasses were dissolved in precleaned Savillex™ Teflon® beakers using 2 mL of 28M HF and 1 mL of 16M HNO_3 and heating on a hotplate at 125 °C for 48 hours. After this initial dissolution stage, the sample was evaporated to dryness and refluxed in 6M HCl in order to break down any fluorides which may have formed. After repeating this process several times, the sample solutions were inspected for visual clarity using an ultraviolet light, and only when no sign of residue was observed, were they evaporated to dryness and taken up in 2.5M HCl prior to column chemistry.

The chemistry and mass spectrometry procedure used here was broadly based on that of Charbonnier et al. (2020). Barium was separated from the sample matrix using a BioRad® PolyPrep™ column loaded with 2mL of cation exchange resin (AG50 X8 200-400 mesh). The resin was precleaned on the column with repeat passes of 6M HCl and MQ H_2O prior to preconditioning with 10 mL of 2.5M HCl. One mL of sample aliquot was loaded onto each column containing approximately 800 ng of Ba. The sample matrix was washed from the resin in 10 mL of 2.5M HCl before the Ba fraction was eluted in 10 mL of 6M HCl. To ensure a good separation of Ba from matrix elements the column separation was repeated twice. The Ba fraction was then evaporated to dryness before being brought back into solution in 0.5M HNO_3, ready for analysis by MC-ICPMS.

Barium isotope measurements were made on the Thermo Scientific Neptune Plus MC-ICPMS instrument at IPGP. The samples were introduced using a 50 μL min^{-1} nebulizer and a SIS quartz spray chamber, with both standards and sample solutions prepared at a concentration of 250 μg/g total Ba which, after tuning, gave a total Ba voltage of 16 V. The masses of $^{129}Xe^+$, $^{130}Ba^+$, $^{132}Ba^+$, $^{134}Ba^+$, $^{135}Ba^+$, $^{136}Ba^+$, $^{137}Ba^+$, $^{138}Ba^+$ and $^{139}La^+$ were collected in faraday cups L4, L3, L2, L1, C, H1, H2, H3 and H4. Standard $10^{11}\Omega$ pre-gain amplifiers were connected to all collectors beside H4 for which a $10^{12}\Omega$ was used. The instrumental mass bias was corrected using the well-established standard-sample bracketing technique, whereby each measurement of a sample is bound by a measurement of the NIST 3104a international standard. Each measurement consisted of 1 block of 50 cycles of 4 second integrations, with each sample aliquot being measured in triplicate as a minimum. Final reported values are the average and 2x standard deviation of the mean and expressed in standard delta notation as per Equation below, where by ^{13X}Ba can represent ^{137}Ba or ^{138}Ba.

$$\delta^{13X/134}Ba\ (‰) = \left(\frac{\left(\frac{^{13X}Ba}{^{134}Ba}\right)_{sample}}{\left(\frac{^{13X}Ba}{^{134}Ba}\right)_{NIST\ 3104a}} - 1 \right) \times 1000$$

Because the chemistry used here does not separate La and Ce well from Ba, the isobaric interference of ^{138}La and ^{138}Ce on ^{138}Ba was large and could not be corrected for using natural abundance. Consequently, we report $\delta^{137/134}$Ba and $\delta^{137/135}$Ba as measured ratios, using them to demonstrate the mass dependency of our technique (see figure below) and provide a

recalculated $^{138/134}$Ba value ($^{138/134}$Ba = 1.33 x $^{137/134}$Ba) for ease of comparison with other Ba isotope studies. The accuracy and precision of the method was assessed by replicate analysis of reference material BHVO-2 (δ^{138}Ba = -0.032±0.032, 2SD).

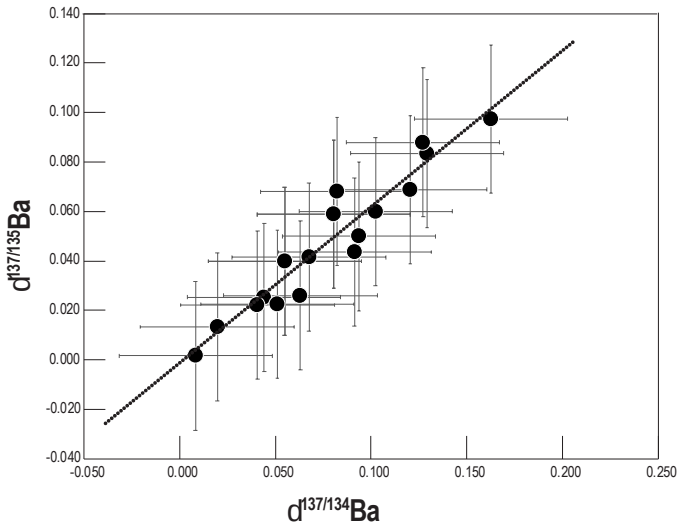

Supplementary figures caption

Supp Figure 1: Radiogenic isotope data obtained in this study on the basanites and phonolites from the various sites between Petite Terre and Fani Maoré. Also shown are data published in the literature for the various Comoros islands (Dupré and Allégre, 1983; Nougier et al., 1986; Späth et al., 1996; Class and Goldstein, 1997; Class et al., 1998; Deniel, 1998; Salters and White, 1998; Class et al., 2005; Pelleter et al., 2014). New data are shown as dots and triangles while published data as downloaded from GeoRoc are shown as diamonds.

Supp Figure 2: Radiogenic isotope data obtained on basanites and phonolites from this study compared to the fields defined by ocean island basalts in general. Published data are compiled from GEOROC database ((https://georoc.eu/) downloaded in 2022.

Supp Figure 3: Barium stable isotopic data obtained in this study on the basanites and phonolites from the various sites between Petite Terre and Fani Maoré. In panel a, data are compared to ranges reported by Charbonnier et al. (2018), Crockford et al. (2019) and Middleton et al. (2023) for various geological materials. For ease the external error (2sd) of the reference material is given, which provides a conservative estimate of the reproducibility of the technique. Panels b and c show how the Ba isotopic composition is unrelated to Ba/Th and to the Sr isotopic composition of the lavas.

Supp Figure 4: Plots of Ce/Pb versus Pb contents in panel (a) and Cu contents in panel (b). In both panels, the element concentration decreases when Ce/Pb ratio increases. While samples from other locations in the Comoros archipelago follow a similar trend for Pb vs Ce/Pb, no clear trend appears for Cu contents.

Supp Figure 5: Plot of Sr/Sr* versus Ba/Th showing that lavas from Fani Maoré have both high Ba/Th and Sr/Sr* while basanites from other locations next to the new volcano have much

lower Ba/Th and Sr/Sr*. Sr/Sr* is calculated as $Sr_N/((Nd_N+Sm_N)/2)$. The normalizing values are those suggested by McDonough and S.S.Sun (1995) for primitive mantle.

Supp Figure 6: Tomographic cross-section of the mantle below Réunion Island, the Comoros Archipelago and the East African Rift Zone (courtesy of Dongmo Wamba et al. (2023) but not published in their paper). The cross section clearly shows that the fast material present under the East African Rift system extends all the way to the Comoros Archipelago.

References

Charbonnier, Q., Bouchez, J., Gaillardet, J., Gayer, É., 2020. Barium stable isotopes as a fingerprint of biological cycling in the Amazon River basin. Biogeosciences, 17(23): 5989-6015.

Charbonnier, Q., Moynier, F., Bouchez, J., 2018. Barium isotope cosmochemistry and geochemistry. Science Bulletin, 63(6): 385-394.

Chauvel, C., Blichert-Toft, J., 2001. A hafnium isotope and trace element perspective on melting of the depleted mantle. Earth and Planetary Science Letters, 190: 137-151.

Chauvel, C., Bureau, S., Poggi, C., 2011. Comprehensive Chemical and Isotopic Analyses of Basalt and Sediment Reference Materials. Geostandards and Geoanalytical Research, 35(1): 125-143.

Class, C., Goldstein, S.L., 1997. Plume-lithosphere interactions in the ocean basins: constraints from the source mineralogy. Earth and Planetary Science Letters, 150: 245-260.

Class, C., Goldstein, S.L., Altherr, R., Bachèlery, P., 1998. The process of plume-lithosphere interactions in the ocean basins-the case of Grande Comore. Journal of Petrology, 39(5): 881-903.

Class, C., Goldstein, S.L., Stute, M., Kurz, M.D., Schlosser, P., 2005. Grand Comore Island: A well-constrained "low 3He/4He" mantle plume. Earth and Planetary Science Letters, 233(3): 391-409.

Crockford, P.W. et al., 2019. Barium-isotopic constraints on the origin of post-Marinoan barites. Earth and Planetary Science Letters, 519: 234-244.

Deniel, C., 1998. Geochemical and isotopic (Sr, Nd, Pb) evidence for plume–lithosphere interactions in the genesis of Grande Comore magmas (Indian Ocean). Chemical Geology, 144(3): 281-303.

Dongmo Wamba, M., Montagner, J.-P., Romanowicz, B., 2023. Imaging deep-mantle plumbing beneath La Réunion and Comores hot spots: Vertical plume conduits and horizontal ponding zones. Science Advances, 9(4): eade3723.

Dupré, B., Allégre, C.J., 1983. Pb-Sr isotope variation in Indian Ocean basalts and mixing phenomena. Nature, 303: 142-146.

Jochum, K.P. et al., 2016. Reference Values Following ISO Guidelines for Frequently Requested Rock Reference Materials. Geostandards and Geoanalytical Research, 40(3): 333-350.

Jochum, K.P. et al., 2011. Determination of Reference Values for NIST SRM 610–617 Glasses Following ISO Guidelines. Geostandards and Geoanalytical Research, 35(4): 397-429.

Luu, T.-H., Gutiérrez, P., Inglis, E.C., Roberts, D., Chauvel, C., 2022. High-precision Sr and Nd isotope measurements using a dynamic zoom lens-equipped thermal ionisation mass spectrometer. Chemical Geology, 611: 121078.

McDonough, W.F., S.S.Sun, 1995. The composition of the Earth. Chemical Geology, 120: 223-253.

Middleton, J.T., Paytan, A., Auro, M., Saito, M.A., Horner, T.J., 2023. Barium isotope signatures of barite–fluid ion exchange in Equatorial Pacific sediments. Earth and Planetary Science Letters, 612: 118150.

Münker, C., Weyer, S., Scherer, E., Mezger, K., 2001. Separation of high field strength elements (Nb, Ta, Zr, Hf) and Lu from rock samples for MC-ICPMS measurements. Geochemistry, Geophysics, Geosystems, 2(12).

Nougier, J., Cantagrel, J.M., Karche, J.P., 1986. The Comores archipelago in the western Indian Ocean: volcanology, geochronology and geodynamic setting. Journal of African Earth Sciences (1983), 5(2): 135-145.

Pelleter, A.-A. et al., 2014. Melilite-bearing lavas in Mayotte (France): An insight into the mantle source below the Comores. Lithos, 208-209: 281-297.

Salters, V.J.M., White, W.M., 1998. Hf isotope constraints on mantle evolution. Chemical Geology, 145: 447-460.

Späth, A., Roex, A.P.L., Duncan, R.A., 1996. The geochemistry of lavas from the Comores archipelago, western Indian ocean: petrogenesis and mantle source region characteristics. Journal of Petrology, 37(4): 961-991.

Thirlwall, M.F., 1991. Long-term reproducibility of multicollector Sr and Nd isotope ratio analysis. Chemical Geology: Isotope Geoscience section, 94(2): 85-104.

White, W.M., Albarède, F., Télouk, P., 2000. High-precision analysis of Pb isotope ratios by multi-collector ICP-MS. Chemical Geology, 167: 257-270.

Supplementary Figure 1

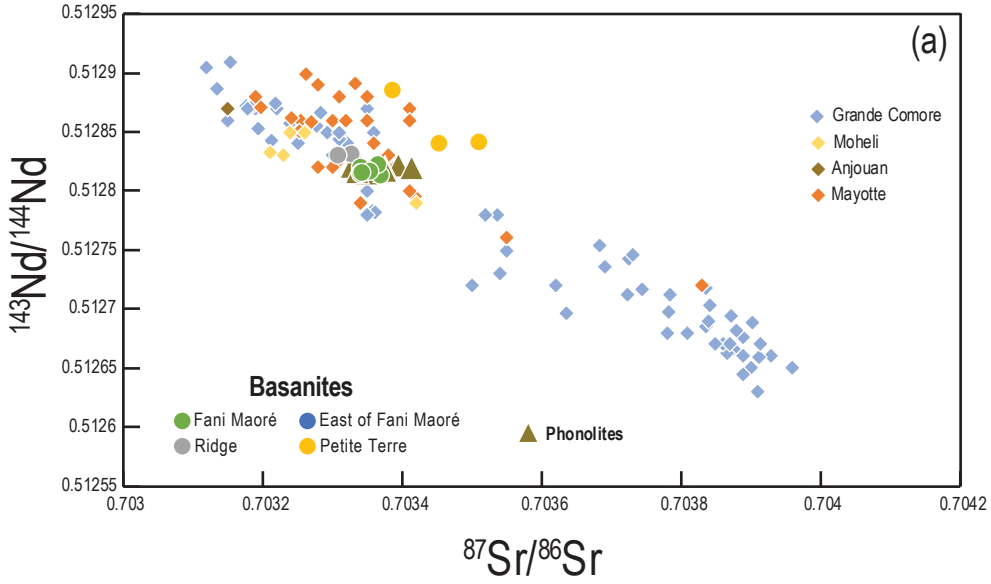

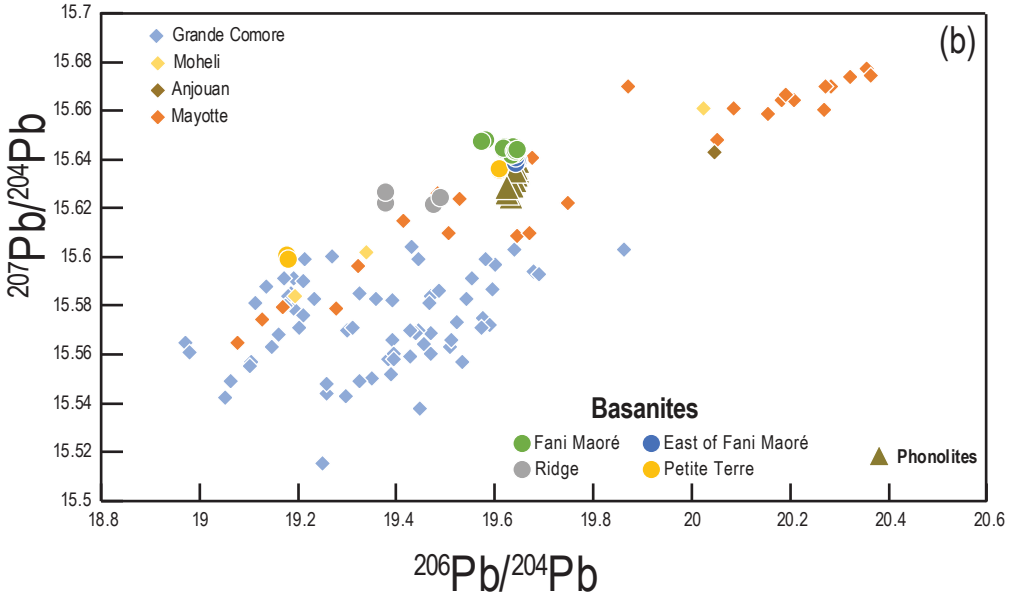

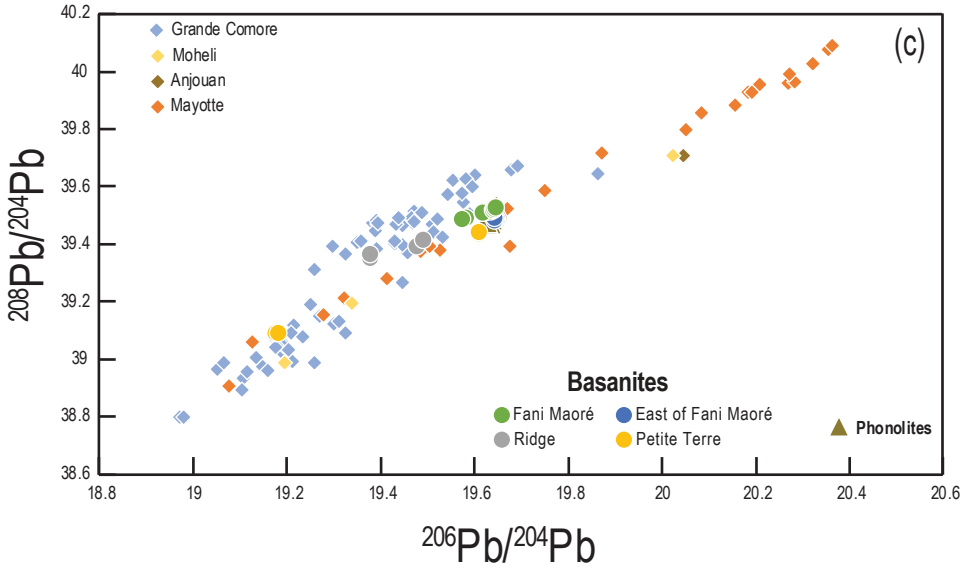

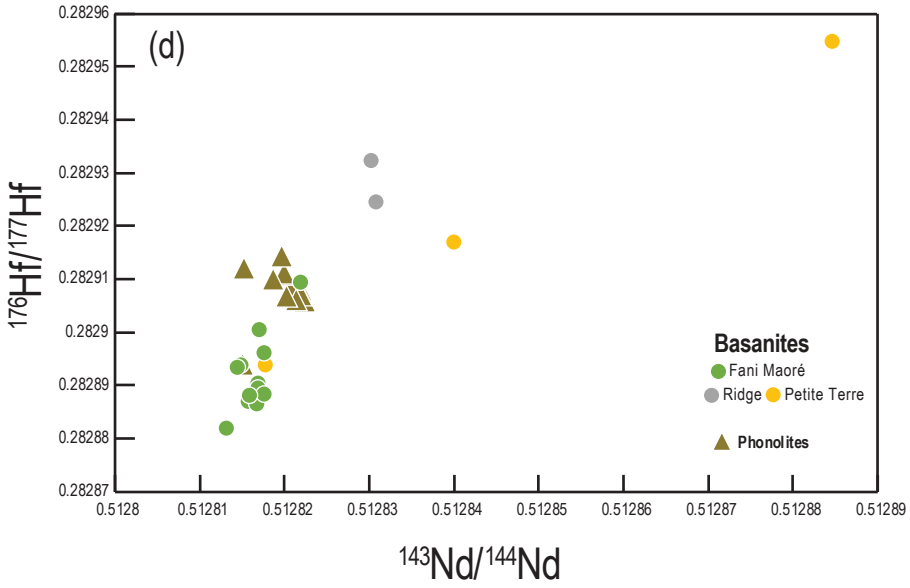

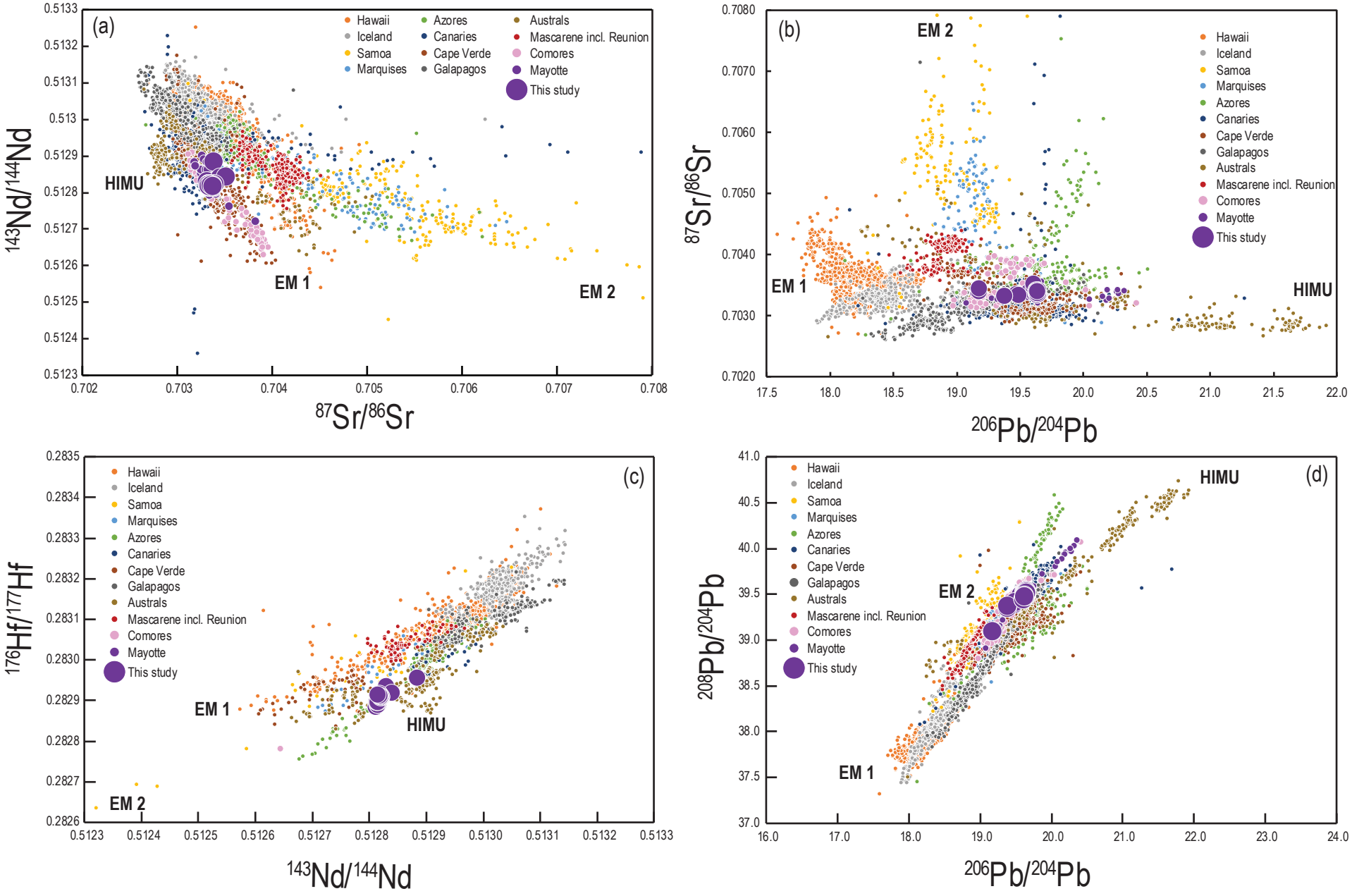
(a)
Hawaii
Iceland
Samoa
Marquises
Azores
Canaries
Cape Verde
Galapagos
Australs
Mascarene incl. Reunion
Comores
Mayotte
This study
HIMU
EM 1
EM 2
143Nd/144Nd
87Sr/86Sr
(b)
EM 2
EM 1
HIMU
87Sr/86Sr
206Pb/204Pb
(c)
EM 1
HIMU
EM 2
176Hf/177Hf
143Nd/144Nd
(d)
HIMU
EM 2
EM 1
208Pb/204Pb
206Pb/204Pb

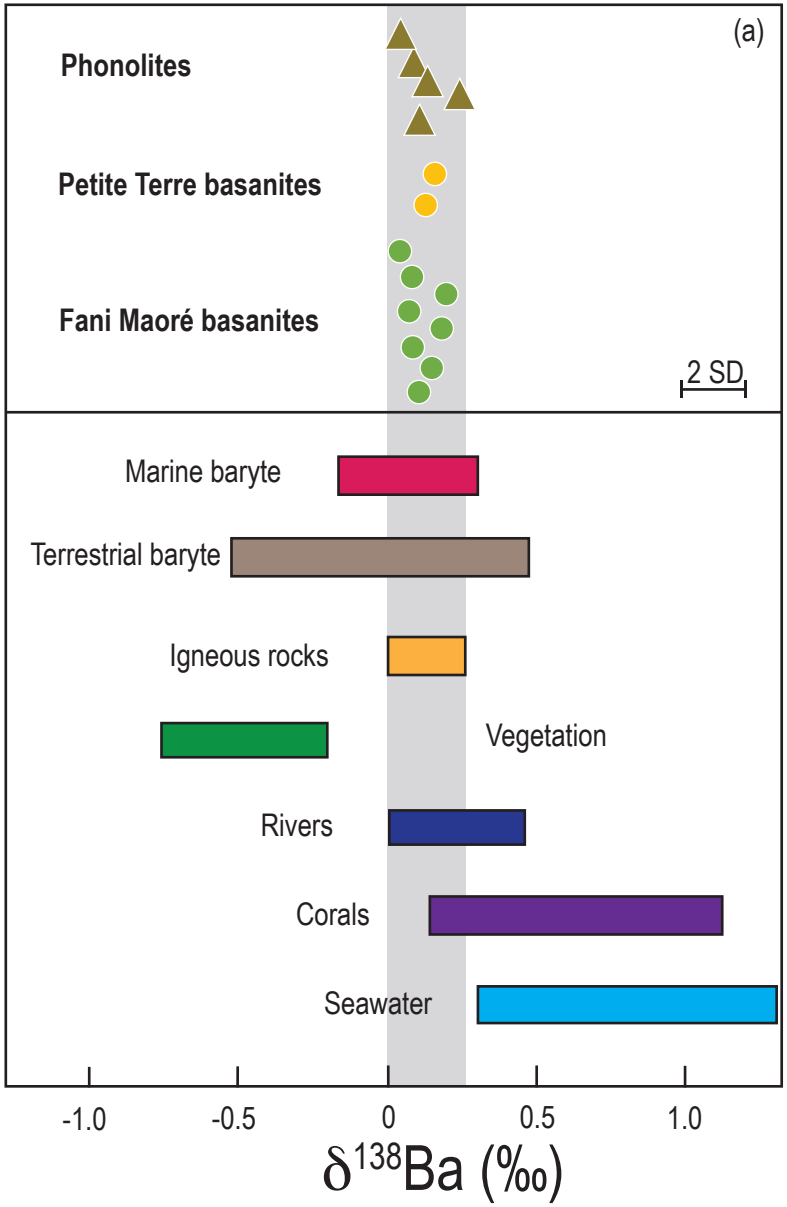
(a)
Phonolites
Petite Terre basanites
Fani Maoré basanites
2 SD
Marine baryte
Terrestrial baryte
Igneous rocks
Vegetation
Rivers
Corals
Seawater
-1.0
-0.5
0
0.5
1.0
δ138Ba (‰)

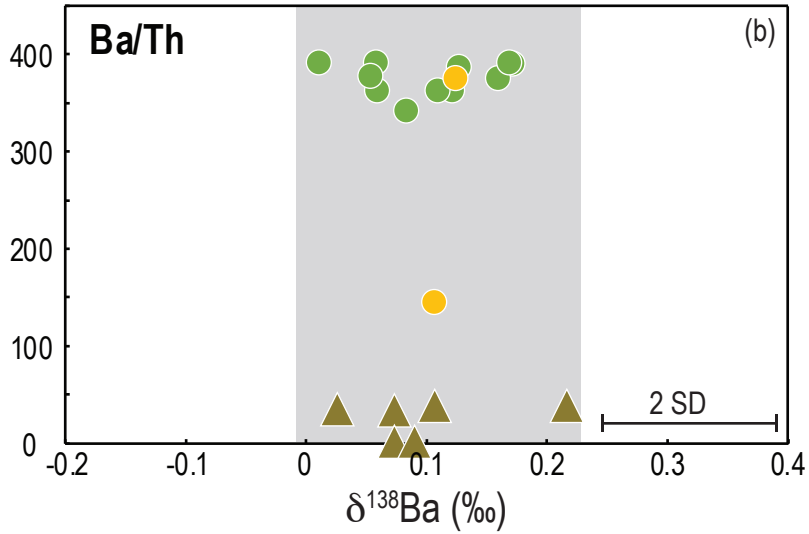
Ba/Th
(b)
400
300
200
100
0
2 SD
-0.2
-0.1
0
0.1
0.2
0.3
0.4
δ138Ba (‰)

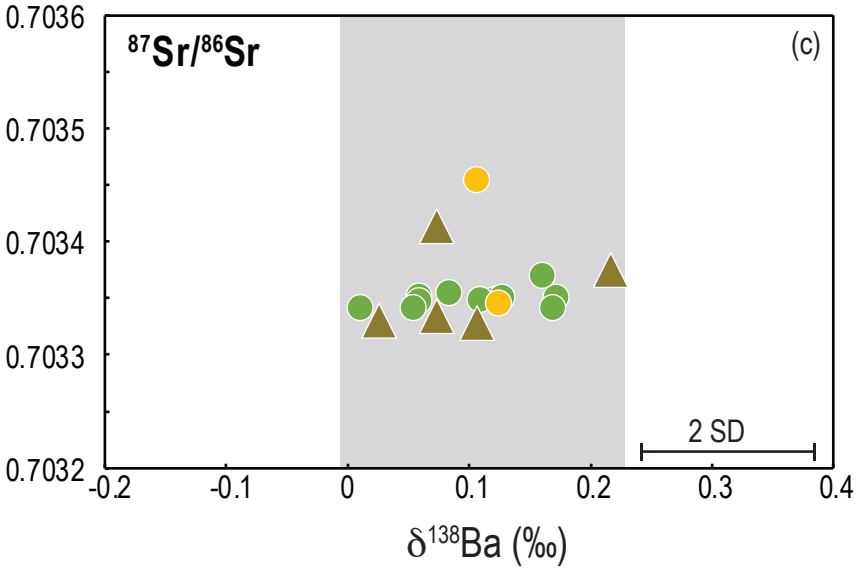
87Sr/86Sr
(c)
0.7036
0.7035
0.7034
0.7033
0.7032
2 SD
-0.2
-0.1
0
0.1
0.2
0.3
0.4
δ138Ba (‰)

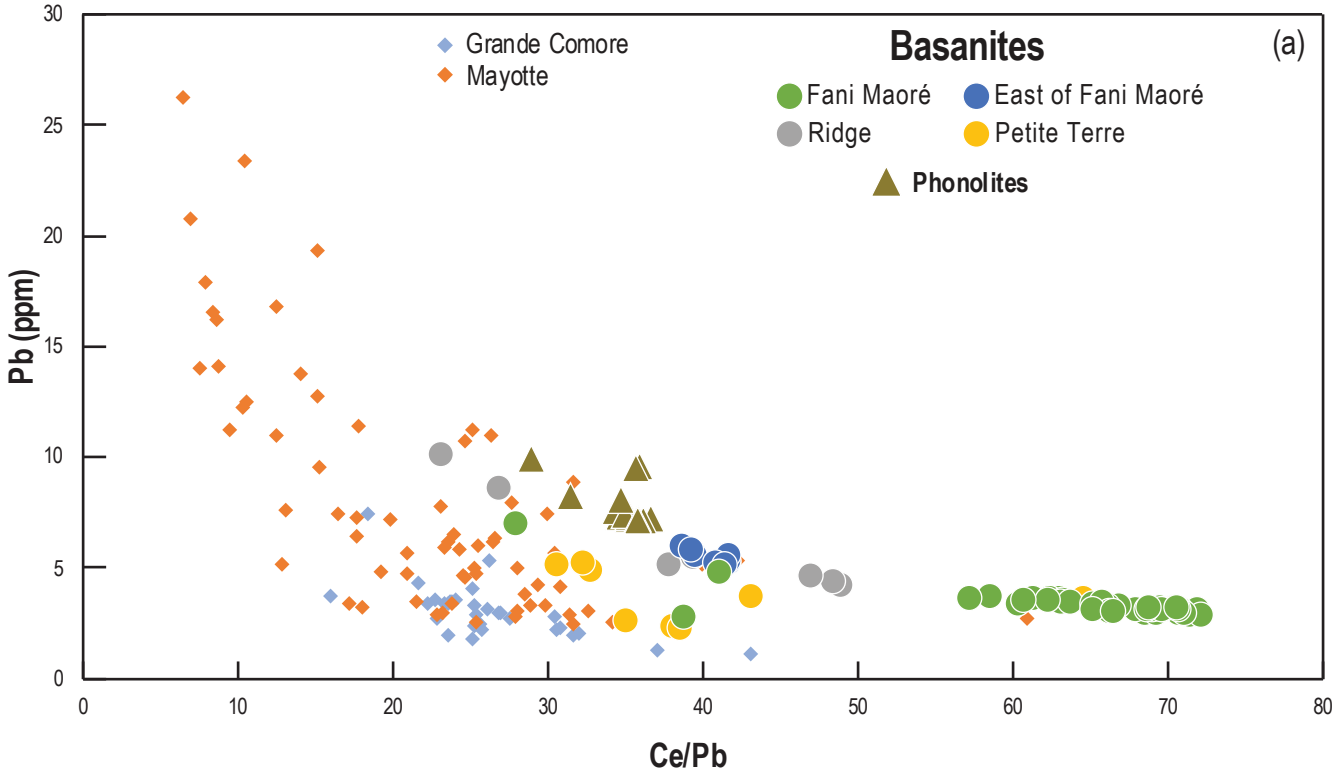
Grande Comore
Mayotte
Basanites
(a)
Fani Maoré
East of Fani Maoré
Ridge
Petite Terre
Phonolites
Pb (ppm)
Ce/Pb
0
5
10
15
20
25
30
0
10
20
30
40
50
60
70
80

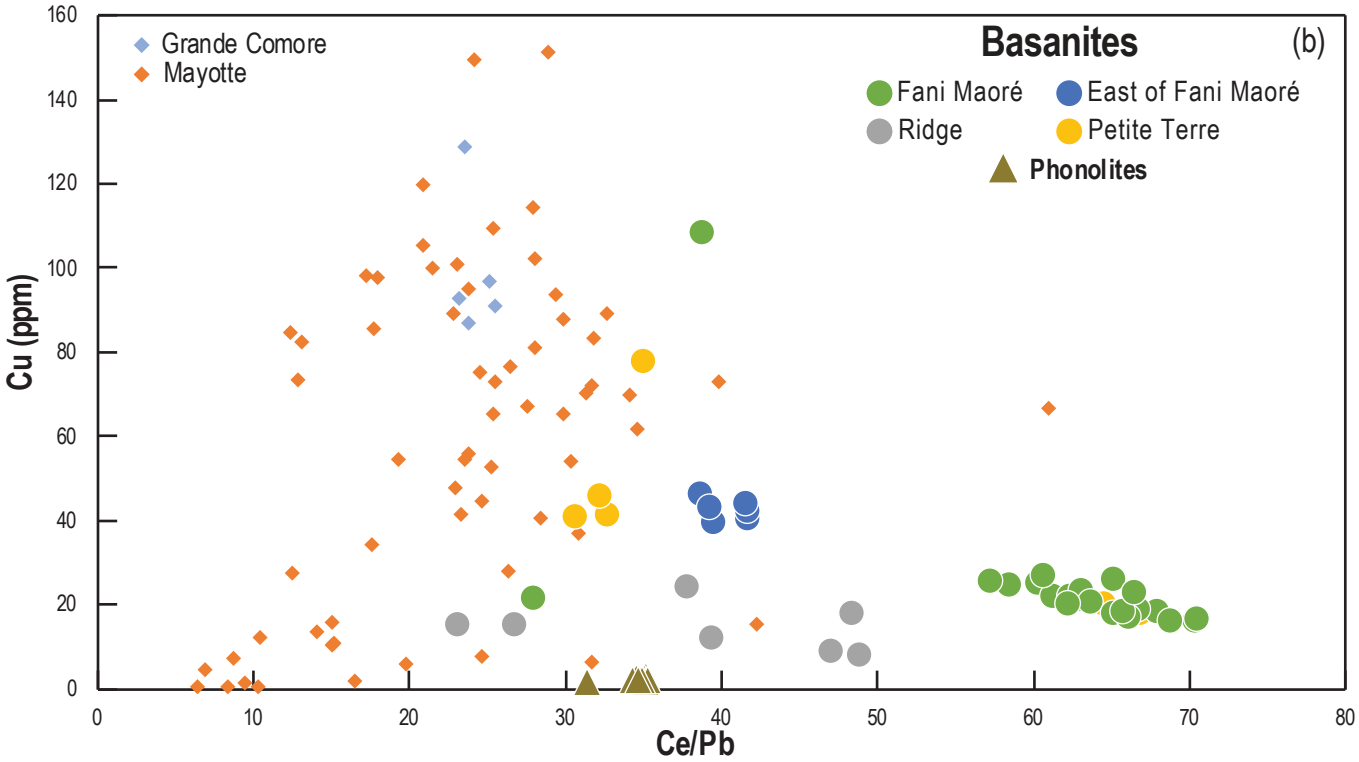
Grande Comore
Mayotte
Basanites
(b)
Fani Maoré
East of Fani Maoré
Ridge
Petite Terre
Phonolites
Cu (ppm)
Ce/Pb
0
20
40
60
80
100
120
140
160
0
10
20
30
40
50
60
70
80

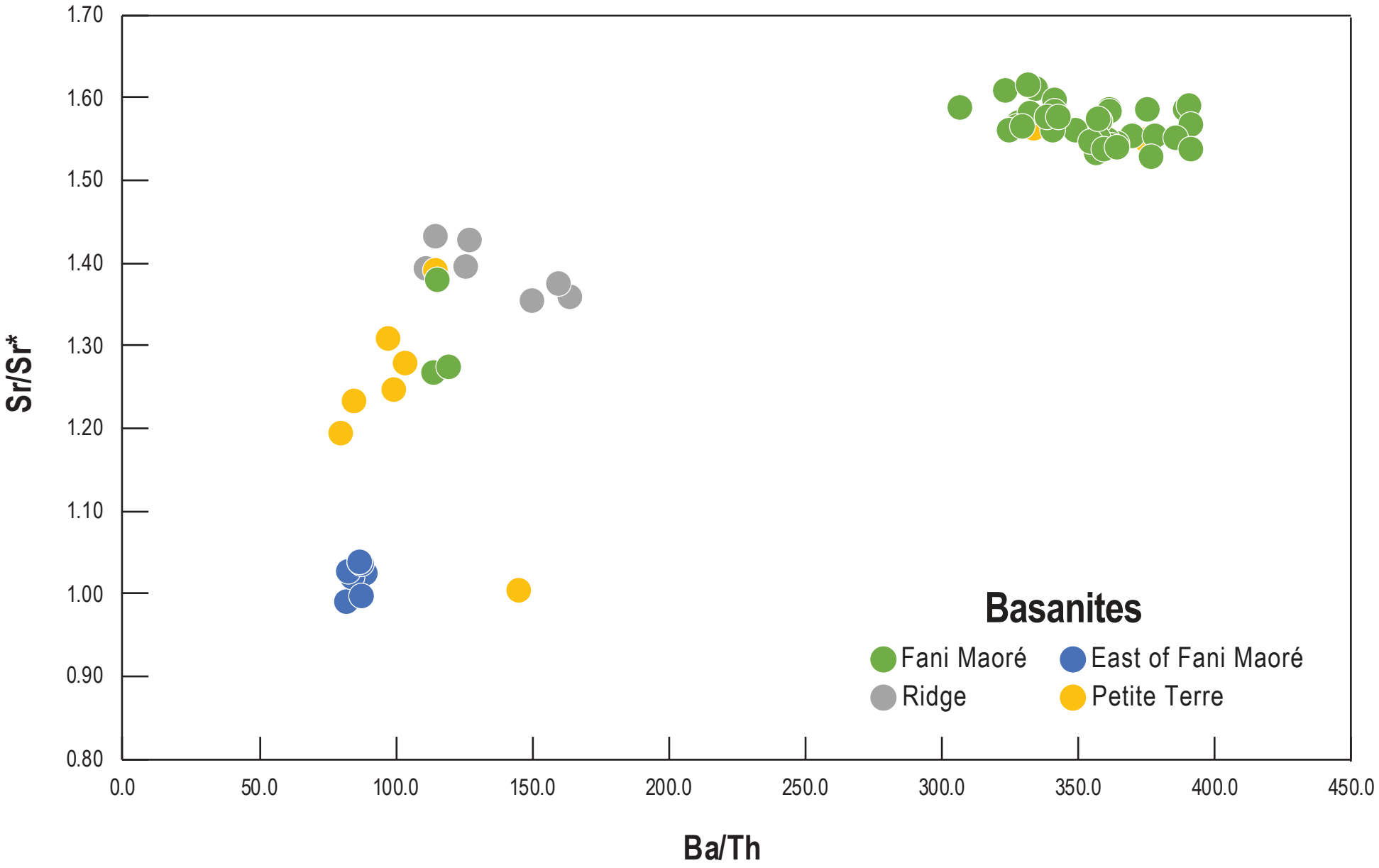
1.70
1.60
1.50
1.40
1.30
1.20
1.10
1.00
0.90
0.80
Sr/Sr*
0.0
50.0
100.0
150.0
200.0
250.0
300.0
350.0
400.0
450.0
Ba/Th
Basanites
Fani Maoré
East of Fani Maoré
Ridge
Petite Terre

Supplementary Figure 6